

# RSC Advances



This is an *Accepted Manuscript*, which has been through the Royal Society of Chemistry peer review process and has been accepted for publication.

*Accepted Manuscripts* are published online shortly after acceptance, before technical editing, formatting and proof reading. Using this free service, authors can make their results available to the community, in citable form, before we publish the edited article. This *Accepted Manuscript* will be replaced by the edited, formatted and paginated article as soon as this is available.

You can find more information about *Accepted Manuscripts* in the [Information for Authors](#).

Please note that technical editing may introduce minor changes to the text and/or graphics, which may alter content. The journal's standard [Terms & Conditions](#) and the [Ethical guidelines](#) still apply. In no event shall the Royal Society of Chemistry be held responsible for any errors or omissions in this *Accepted Manuscript* or any consequences arising from the use of any information it contains.

# Porous elastomeric polyurethane monolith synthesized by concentrated emulsion templating and its pressure-sensitive conductive property

Xiaoqian Zhang,<sup>1,2</sup> Zhongjie Du,<sup>1</sup> Wei Zou,<sup>1</sup> Hangquan Li,<sup>1</sup> Chen Zhang,<sup>1\*</sup> Shuxin Li<sup>2</sup> and Wenli Guo<sup>2\*</sup>

1. Key Laboratory of Carbon Fiber and Functional Polymers (Beijing University of Chemical Technology), Ministry of Education; College of Materials Science and Engineering, Beijing University of Chemical Technology, Beijing 100029, China

2. Beijing Key Lab of Special Elastomeric Composite Materials (Beijing Institute of Petrochemical Technology); Department of Material Science and Engineering, Beijing Institute of Petrochemical Technology, Beijing 102617, China

## Abstract

Porous elastic and pressure-sensitive conductive polyurethane (PU) monoliths were synthesized by concentrated emulsion templating. A toluene solution containing tolylene diisocyanat (TDI), castor oil, and a surfactant was used as the continuous phase of the concentrated emulsion, and deionized water was used as the dispersed phase. In order to make the monolith conductive, acid-treated multi-walled carbon nanotubes (MWCNTs) was introduced into, which were distributed in both phases spontaneously. After the continuous phase of the concentrated emulsion was cured, toluene and water were removed, a highly porous elastic monolith was obtained. The MWCNTs in the continuous phase was embedded in the bulk PU matrix forming a conductive network and those previously in the dispersed phase were precipitated on the surface of the pore wall. It was the touch degree of the MWCNTs on the pore wall rendered the monolith with pressure-sensitive conductivity. A compression strain about 40% could cause a reduction of resistance by two orders of magnitude.

**Keywords:** porous elastic polyurethane; concentrated emulsion; resistance; acid-treated MWCNTs; pressure-sensitive conductive material

---

\*Corresponding authors: [zhangch@mail.buct.edu.cn](mailto:zhangch@mail.buct.edu.cn) (C. Zhang), [gwenli@bipt.edu.cn](mailto:gwenli@bipt.edu.cn) (W. Guo)

## Introduction

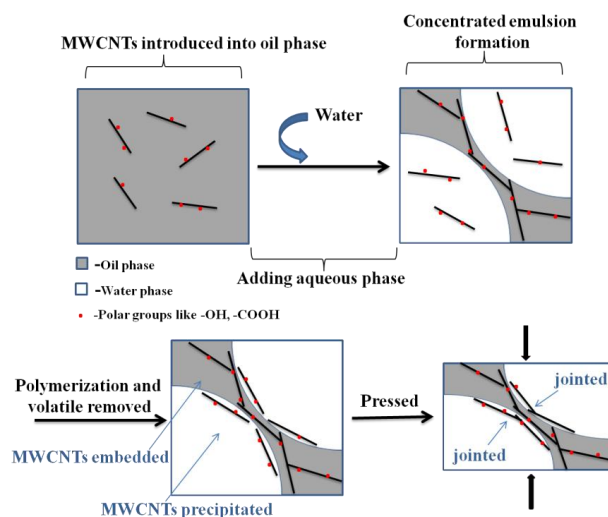
Concentrated emulsions are commonly defined as inverse emulsions (w/o) in which the dispersed phase occupies at least 74% of the volume; this corresponds to the maximum packaging fraction of monodispersed droplets<sup>1-5</sup>. In this system, the dispersed phase is usually an aqueous medium and the continuous phase contains one or more monomers. After the continuous phase polymerized and the dispersed phase is removed, a porous monolith remains. In addition, the porous polymer prepared by concentrated emulsion template usually possesses a partial or full open-cell structure. The interest in these porous monoliths is driven by a large number of applications like catalytic supports<sup>6</sup>, electrochemical sensors<sup>7</sup>, and scaffolds for tissue engineering<sup>8-14</sup>.

Despite of the simplicity of its preparation, the curing of the continuous phase are limited to chain polymerization, with the majority being free radical polymerization of vinyl monomers<sup>5, 15-16</sup>. Polycondensation was seldom tried because the functional groups on the monomers may be highly harmful to the stability of the concentrated emulsions. Furthermore, porous monoliths so far synthesized by concentrated emulsion templating are hard and brittle, few reports are about elastic or flexible porous polymers<sup>3, 17-25</sup>.

Polyurethane (PU) elastomer has received considerable attention in recent years, because of their excellent mechanical properties, abrasion resistance, high flexibility, damping property, and good biocompatibility<sup>26-35</sup>. In many applications, a porous structure of the PU elastomer is necessary for their biocompatibility and biodegradability<sup>36-41</sup>. However, at present, the elastic PU foams were mainly free-rise PU foams which are obtained from the simultaneous reaction of a polyisocyanate with polyols and water and the porous structure is formed by a gas liberation (foaming). With such technology, the pore size and its distribution are not controllable. Therefore, concentrated emulsion templating is doubtless a suitable way to control the morphology and pore structure of the elastic PU foam.

The purpose of controlling porous structure in PU elastomer in general may be to manipulate its mechanical properties, damping behavior, or biomedical performance. Distinctively, this study is aimed to adjust the conductive property. As commonly practiced, acid-treated multi-walled carbon nanotubes (MWCNTs) were introduced as conductive filler,

because of their higher conductivity and larger aspect ratio<sup>42-43</sup>, and PU elastomer with controlling porous structure was fabricated by concentrated emulsion templating. The MWCNTs were firstly acid-treated to improve the dispersion in PU matrix. Interestingly, in the preparation of the concentrated emulsion templating, a spontaneously distribution of the acid-treated MWCNTs would be achieved and lead to a strain-response conductivity. The MWCNTs in the continuous phase was embedded in the bulk PU matrix forming a conductive network and those previously in the dispersed phase were precipitated on the surface of the pore wall. Therefore, the conductivity of a highly compressible material could be tuned with applied pressure. The compression would facilitate the MWCNTs on the pore wall to cross through the interconnecting macropores and come close to each other. As a result, the conductivity of the foam would increase obviously (Scheme 1). To the best of our knowledge, this study is the first on the pressure-sensitive conductive PU monolith with a uniform porosity by concentrated emulsion templating. The obtained elastic press-sensitive conductive foam has the potential application on biosensors, electromagnetic interference (EMI) shielding, and fuel cell membranes<sup>44-47</sup>.



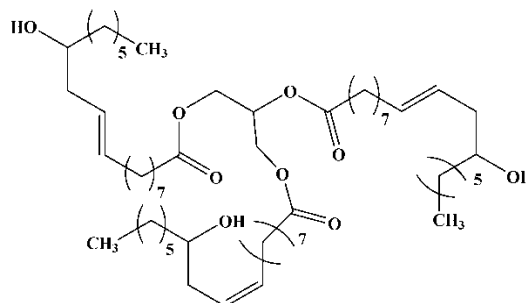
Scheme 1. Formation of press-sensitive conductive porous PU.

## Experimental

### Materials

Toluene diisocyanate (TDI) was supplied by Tianjing Chemical Co., China. Castor oil was purchased from Inner Mongolia Weiyu Biological Technology Co., Ltd. Multi-walled carbon nanotubes (MWCNTs) with purity >95%, 10-30 nm diameter and 0.5-500  $\mu\text{m}$  length

were supplied by Shenzhen Nanotech Port, China. Polyglycerol polyricinoleate (PGPR,  $C_{57}O_9H_{104}$ ) was bought from Henan Tianrun Biological Technology Co., Ltd, and its structure was illustrated in Scheme 2. Toluene was provided from Xilong chemical Co., Ltd.



Scheme 2. The structure of PGPR

### Preparation of acid-treated MWCNTs

The raw MWCNTs were dispersed in concentrated sulfuric acid for 24 h, then refluxed in the mixture of concentrated acids ( $HNO_3/H_2SO_4=1/1$ , vol/vol) at  $140^\circ C$  for 30 min. The oxidized MWCNTs were washed with the de-ionized water until the filtrate was neutral.

### Preparation of porous PU monolith

The organic phase, the mixture of toluene 1.496g, TDI 1.742g, castor oil 3.388g, and PGPR 1.575g, was put into a 100ml round-bottomed flask equipped with a high-speed stirrer. In the preparation of conductive monolith, acid-treated MWCNTs were also introduced into the organic phase. The aqueous phase (de-ionized water) was slowly added dropwise to the continuous phase through an injector under a mechanical stirring of 200 rpm until a certain volume fraction was reached. The addition of the latter lasted about 30 min and a milky concentrated emulsion was obtained.

The concentrated emulsion was transferred to glass test tube, sealed, and then put into a vacuum oven at  $70^\circ C$  for 6 hours to complete the curing. After the volatile species were removed, a porous PU monolith was obtained.

### Characterization

The morphology of porous PU monolith was characterized by scanning electron microscopy (SEM, S-4700, JEOL Ltd., Tokyo, Japan) instrument operated at an accelerating voltage of 20 kV. The resistance of porous PU monolith was characterized through a digital hand-hold multimeter (VC9801A<sup>+</sup>, VICTOR, Guangdong, China) and a super-high resistance

meter (ZC43, Shanghai, China). Apparent densities of the porous monolith were calculated from the weight and the physical dimensions of the samples according to GB/T6343-1995 and in each group five samples were taken into account. Thermo-gravimetric analysis (TGA, Netzsch TG 209c) was conducted at a heating rate of 10 °C/min from room temperature to 700 °C under nitrogen.

## Results and discussion

### Influence of the surfactant concentration on the porous morphology

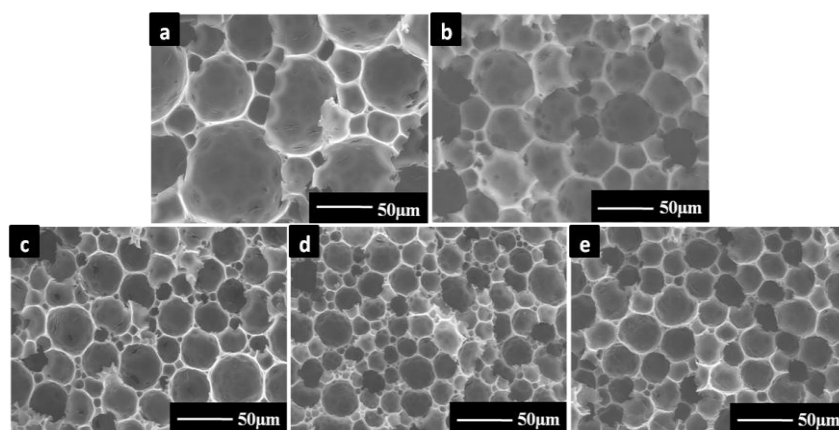


**Figure 1.** SEM images of porous PU monolith with different surfactant concentrations: (a) 1.9, (b) 3.8, (c) 7.6, (d) 15.2, (e) 22.8 wt% of the continuous phase. Toluene was 26 wt% of the continuous phase; Castor oil was 42.5 wt% of the continuous phase; The dispersed phase was 75 vol%.

In order to maintain the stability of the concentrated emulsion, a reactive surfactant PGPR was employed in this work. From Scheme 2, each PGPR molecule possesses three –OH groups, and for this reason it may participate the curing reaction with TDI. This reaction may thicken the interface between the two phases and strengthen the barrier to block the reaction between TDI and water, and inhibit the coagulation of the aqueous droplets, and thus made the porous structure finer<sup>48</sup>.

The SEM micrographs based on various surfactant concentrations were presented in Figure 1. It was found that the average pore size kept decreasing with increasing PGPR content until it was 15.2 wt% relative to the amount of the continuous phase. When the PGPR content increased from 15.2 to 22.8 wt%, the average pore size stopped decreasing, however,

the pore structure became more uniform. This behavior demonstrated that the concentration of 15.2 wt% was enough to maintain the stability of the concentrated emulsion and kept the dispersed droplets from coalescence. However, the porous structure was non-uniform. At higher PGPR content of 22.8 wt%, an excess reaction heat would be generated, and the system would be locally over-heated. As a result, localized coalescence of droplets would occur, especially for those with small sizes. This effect would finally lead to more uniform porous structure.

### Influence of the amount of castor oil on the porous morphology

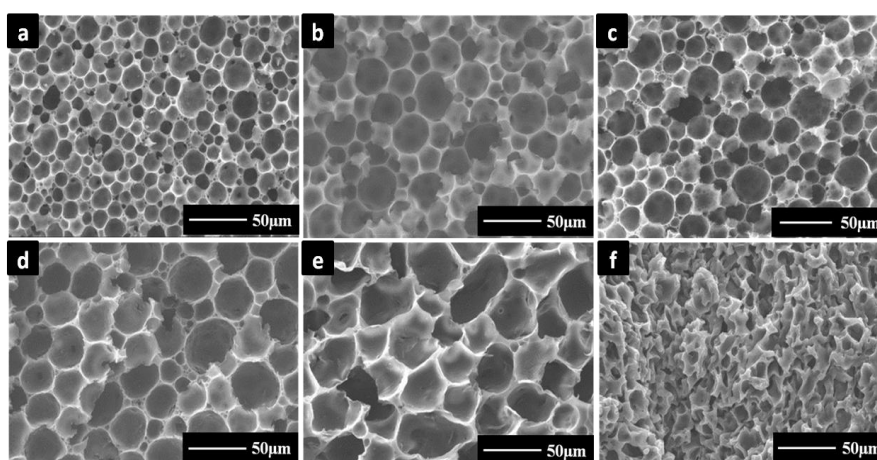


**Figure 2.** SEM images of porous PU monolith with different amount of castor oil: (a) 0; (b) 17.0; (c) 34.0; (d) 42.5; (e) 51.0; (f) 59.5 wt% of the continuous phase. Toluene was 26 wt% of the continuous phase; PGRP was 22.8 wt% of the continuous phase; The dispersed phase was 75 vol%.

The bulk of PU monolith in this work was formed essentially from the reaction between TDI and castor oil, although the reaction between TDI and the reactive surfactant PGPR may also be taken in account. Since the castor oil constituted the soft segments of the PU network, the content of castor oil would be the predominant factor for the stiffness and the porous structure of the monolith.

The SEM images in Figure 2 presented the porous structure of the PU monolith derived from various castor oil contents. One may notice that when the content of castor oil was low (Figure 2a~d), the PU network was somewhat rigid and the morphologies of the

concentrated emulsion precursor could be maintained, most of the pores left by the aqueous droplets were spherical. However, it could be found that the size of the pores became larger with the increasing content of castor oil. Because the higher the content of castor oil, the less the ability of the pore wall to inhibit the coagulation, and the larger final pores were generated. When the content of castor oil was 51.0 wt% (Figure 2e), the pore wall became so flexible that the pores were deformed and deviated from spherical shape. Further increasing the castor oil content to 59.5 wt% (Figure 2f), the pore wall lost the rigidity and became collapsed. A different type of pore structure with small and irregular pores was observed. The collapse of the pore wall made the PU foam denser and shortened the distance among them, which, as will be clear later, provided a necessary structure for the pressure-sensitive conductivity.

### Influence of acid-treated MWCNTs on the pore structure

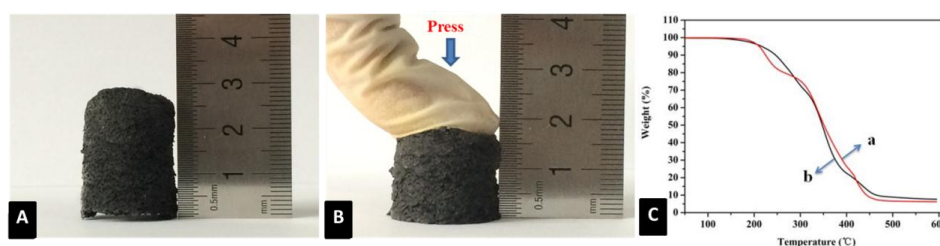


**Figure 3.** Photographs of (A) pristine PU/MWCNTs monolith, and (B) pressed PU/MWCNTs monolith; (C) TGA curves of porous PU monoliths with (a) free MWCNTs, (b) 2 wt% MWCNTs.

In order to make the PU monolith conductive, MWCNTs were introduced into the concentrated emulsion. After the curing reaction of the continuous phase and removal of the volatile species, a black and elastomeric PU monolith was obtained (Fig 5. (A) and (B)). Moreover, it could be found from TGA curves that the weight loss at 500 °C of the porous PU monolith without MWCNTs was 91.49% and that of the sample with 2 wt% MWCNTs were 93.47% (Fig 5.(C)). The 1.98wt% of difference value agreed with the weight of the introduced MWCNTs. The densities of the PU porous monoliths with different amount of acid-treated MWCNTs were listed in Table 1. The plenty of micropores contributed the lower density and then lighter weight of the monolith. Compared with the PU porous monoliths without MWCNTs, the densities increased a little with the introduction of MWCNTs. All the



results identified that the elastomeric polymer foam was obtained and the MWCNTs were successfully introduced into.

Table 1. The densities of PU porous monoliths with different amount of MWCNTs.

MWCNTs content (wt %)	0.00	0.75	1.00	2.00
densities (g/cm <sup>3</sup> )	0.193	0.249	0.257	0.265

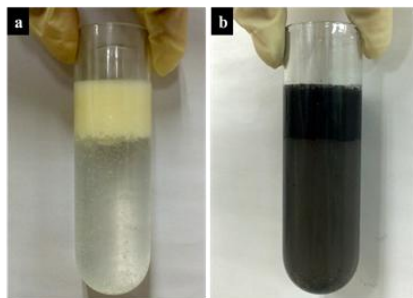


**Figure 4.** Pictures of the unstable concentrated emulsions: (a) acid-treated MWCNTs free, (b) acid-treated MWCNTs present. Castor oil was 59.5 wt % of the continuous phase; Toluene was 26 wt% of the continuous phase; PGPR was 22.8 wt% of the continuous phase; The dispersed phase was 75 vol%; The mass fraction of acid-treated MWCNTs was 1.0 wt% of the continuous phase.

The MWCNTs used in this work was pre-treated with HNO<sub>3</sub>/H<sub>2</sub>SO<sub>4</sub> acids, and bore some polar groups like -OH, -COOH, -C=O on the surface<sup>49-51</sup>. As a result, the MWCNTs were hydrophobic in bulk and somewhat hydrophilic on the surface. For this reason the MWCNTs could be dispersed in both oil continuous and aqueous dispersed phases. Figure 4 showed that the distribution of MWCNTs in the two liquids used as the continuous and dispersed phases of a concentrated emulsion, the upper layer was the oil phase and the lower the deionized water. Without MWCNTs, the oil phase was milky and water was transparent. After the MWCNTs were introduced, the oil phase became black and water became dark, which indicated that the solubility of the MWCNTs in two phases was not equal. A quantitative measurement showed that about 74.6 wt% of the MWCNTs was in the continuous phase and the rest in the dispersed phase.

Although the MWCNTs were introduced a few percentages, the property of the

concentrated emulsion might be changed. First of all, the viscosity of both phases could be a little increased, which was favorable to the kinetic stability of the system. In other hand, the MWCNTs were hydrophobic in bulk and hydrophilic on the surface, which may be harmful to the stability. The balance of the two effects could be detected from the porous morphology of the final monolith, which was presented in Figure 5. Figure 5a was the SEM micrograph for the sample default of the MWCNTs, and Figure 5b and c were those containing 1.0 and 1.5 wt% MWCNTs. A comparison among Figure 5a through c, one may generally tell that no obvious change was detected.

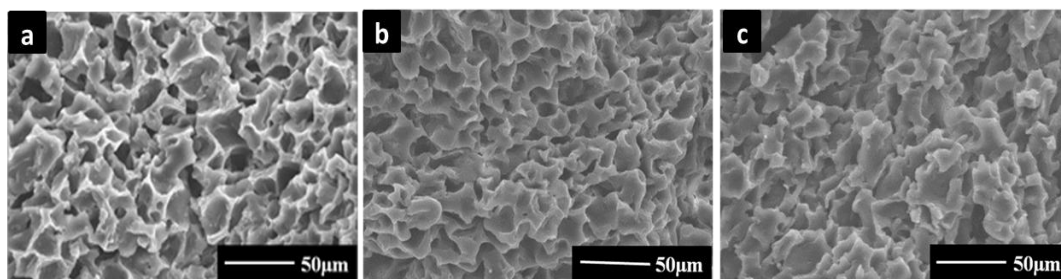


**Fig 5.** SEM images of porous PU monolith with different amount of acid-treated MWCNTs: (a) 0.0, (b) 1.0, (c) 1.5 wt%. Castor oil was 59.5 wt % of the continuous phase; Toluene was 26 wt% of the continuous phase; PGRP was 22.8 wt% of the continuous phase; The dispersed phase was 75 vol%.

#### Influence of acid-treated MWCNTs on the resistance of porous PU monolith

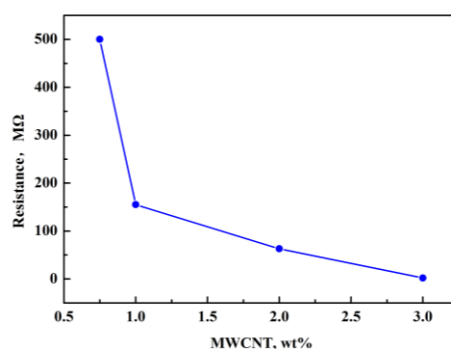


**Figure 6.** Influence of the amount of loaded MWCNTs on the resistance of PU monoliths. Castor oil was 59.5 wt % of the continuous phase; Toluene was 26 wt% of the continuous phase; PGRP was 22.8 wt% of the continuous phase; The dispersed phase was 75 vol%.

As discussed above, the major part of MWCNTs was presented in the oil phase and after

curing of the concentrated emulsion, was embedded in the pore-wall; and the rest MWCNTs was first in the dispersed aqueous droplets, after the water removal, would precipitate on the surface of the pore-wall. With such a structure, the monolith was conductive because the MWCNTs in the bulk formed a continuous network, the MWCNTs on the surface made a little contribution to the conductivity.

The influence of the amount of MWCNTs loading on the resistance of porous PU was presented in Figure 6. As expected, the resistance of PU monolith decreased with increasing amount of MWCNTs. When the mass fraction of the MWCNTs was 0.75 wt%, the resistance was as high as 500 M $\Omega$ , and this value decreased sharply to 155 M $\Omega$  as the MWCNTs loading became 1.0 wt%. Thereafter, the change in resistance became flattened but still kept decreased. When the content of MWCNTs increased to 3.0 wt%, the resistance of the monolith was only 2 M $\Omega$ . In other words, a decrease of two orders of magnitude was observed.

#### Influence of compression strain on the resistance of porous PU monolith

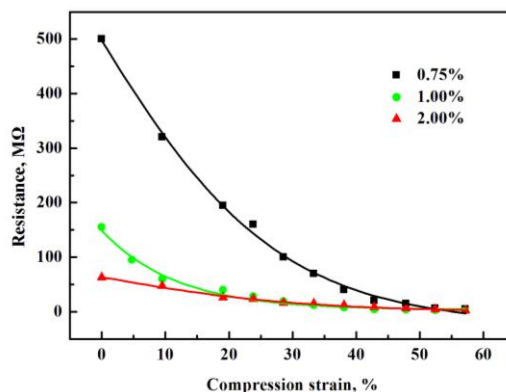


**Figure 7.** Influence of compression strain of porous PU monolith on the resistance (mass fraction of acid-treated MWCNTs: 0.75wt%, 1.00wt%, 2.00wt%). Castor oil was 59.5 wt % of the continuous phase; Toluene was 26 wt% of the continuous phase; PGRP was 22.8 wt% of the continuous phase; The dispersed phase was 75 vol%.

When a pressure was applied on the PU monolith, it would deform and make the MWCNTs better touched, thus decreased the resistance. Using the lowest MWCNTs content, 0.75 wt%, the effect of compression strain on the resistance was shown in Figure 7. When the

compression strain was less than 40%, the resistance of PU monolith decreased sharply with increasing compression strain, a decrease about two orders of magnitude was observed. Further increasing the compression strain, the resistance leveled off. This meant that a compression strain about 40% was enough to make the MWCNTs sufficiently touched each other and provide a low resistance. However, the critical compression strain was depended on the content of MWCNTs, the higher the MWCNTs content, the lower the critical compression strain. When the higher content of MWCNTs was introduced, some MWCNTs on the surface might percolate, which lead to improved conductivity but weakened pressure-sensitive of the PU monolith, as shown in Figure 7.

## Conclusions

Porous elastic PU monolith with a pressure-sensitive conductivity was prepared by concentrated emulsion templating. Acid-treated MWCNTs was introduced into the precursor concentrated emulsion, the major part of MWCNTs was present in the continuous phase forming a conductive network, the rest of MWCNTs would dispersed in the aqueous droplets and would precipitate on the surface of the pore wall of the monolith after the removal of the dispersed phase, which constituted an additional path for applied current. When the monolith was subjected to compression, the MWCNTs accumulated on the surface contacted each other and further decreased the resistance. As a result, the monolith was pressure conductive sensitive and could be used as a pressure sensor.

## Acknowledgements

This work is supported by Innovation Promotion Project of Beijing Municipal Commission of Education, China (TJSHG201310017034) and the 13th CHINA-JAPAN S and T Cooperation (2010DFA52070).

## References

- 1 R. Mezzenga, J. Ruokolainen, G. H. Fredrickson and E. J. Kramer, *Macromolecules*, 2003, **36**,

- 4466-4471.
- 2 N. R. Cameron, *Polymer*, 2005, **46**, 1439-1449.
- 3 N. Cameron and D. Sherrington, *J. Mater. Chem.*, 1997, **7**, 2209-2212.
- 4 N. R. Cameron, D. C. Sherrington, I. Ando and H. Kurosu, *J. Mater. Chem.*, 1996, **6**, 719-726.
- 5 M. S. Silverstein, *Prog. Polym. Sci.*, 2014, **39**, 199-234.
- 6 S. Kovačič, A. Anžlovar, B. t. Erjavec, G. Kapun, N. B. Matsko, M. Žigon, E. Žagar, A. Pintar and C. Slugovc, *ACS Appl. Mater. Interfaces*, 2014, **6**, 19075-19081.
- 7 C.-X. Yuan, Y.-R. Fan, H.-X. Guo, J.-X. Zhang, Y.-L. Wang, D.-L. Shan and X.-Q. Lu, *Biosens. Bioelectron.*, 2014, **58**, 85-91.
- 8 A. Barbetta, M. Dentini, M. S. De Vecchis, P. Filippini, G. Formisano and S. Caiazza, *Adv. Funct. Mater.*, 2005, **15**, 118-124.
- 9 A. Barbetta, M. Dentini, E. M. Zannoni and M. E. De Stefano, *Langmuir*, 2005, **21**, 12333-12341.
- 10 S. Bhunia, N. Chatterjee, S. Das, K. Das Saha and A. Bhaumik, *ACS Appl. Mater. Interfaces*, 2014, **6**, 22569-22576.
- 11 R. M. Domingues, M. E. Gomes and R. L. Reis, *Biomacromolecules*, 2014, **15**, 2327-2346.
- 12 M. S. Kim and G. Kim, *Langmuir*, 2014, **30**, 8551-8557.
- 13 X. Liu, K. Zhao, T. Gong, J. Song, C. Bao, E. Luo, J. Weng and S. Zhou, *Biomacromolecules*, 2014, **15**, 1019-1030.
- 14 D. W. Johnson, C. R. Langford, M. P. Didsbury, B. Lipp, S. A. Przyborski and N. R. Cameron, *Polym. Chem.*, 2015.
- 15 A. Imhof and D. J. Pine, *Advanced Materials*, 1998, **10**, 697-700.
- 16 R. Butler, C. M. Davies and A. I. Cooper, *Advanced Materials*, 2001, **13**, 1459-1463.
- 17 N. R. Cameron and A. Barbetta, *J. Mater. Chem.*, 2000, **10**, 2466-2471.
- 18 J. M. Williams, A. J. Gray and M. H. Wilkerson, *Langmuir*, 1990, **6**, 437-444.
- 19 K. Haibach, A. Menner, R. Powell and A. Bismarck, *Polymer*, 2006, **47**, 4513-4519.
- 20 A. Barbetta, M. Dentini, L. Leandri, G. Ferraris, A. Coletta and M. Bernabei, *Reactive and Functional Polymers*, 2009, **69**, 724-736.
- 21 N. Cohen and M. S. Silverstein, *Polymer*, 2011, **52**, 282-287.
- 22 P. Krajnc, J. F. Brown and N. R. Cameron, *Org. Lett.*, 2002, **4**, 2497-2500.
- 23 M. S. Silverstein, H. Tai, A. Sergienko, Y. Lumelsky and S. Pavlovsky, *Polymer*, 2005, **46**, 6682-6694.
- 24 Y. Tunc, N. Hasirci and K. Ulubayram, *Soft Materials*, 2012, **10**, 449-461.
- 25 A. Menner, K. Haibach, R. Powell and A. Bismarck, *Polymer*, 2006, **47**, 7628-7635.
- 26 S. Gogolewski, K. Gorna, E. Zaczynska and A. Czarny, *J. Biomed. Mater. Res. Part A*, 2008, **85**, 456-465.
- 27 Z. J. Dou, M. Cheng, Y. F. Qin, L. Chen and Z. Y. Qin, *Adv. Mater. Res. Trans Tech Publ*: 2014, 249-253.
- 28 J. Dutta and K. Naskar, *RSC Adv.*, 2014, **4**, 60831-60841.
- 29 B. Li, M. Li, C. Fan, M. Ren, P. Wu, L. Luo, X. Wang and X. Liu, *Compos. Sci. Technol.*, 2015, **106**, 68-75.
- 30 S.-H. Ye, Y. Hong, H. Sakaguchi, V. Shankarraman, S. K. Luketich, A. D'Amore and W. R. Wagner, *ACS Appl. Mater. Interfaces*, 2014, **6**, 22796-22806.
- 31 E. Bat, Z. Zhang, J. Feijen, D. W. Grijpma and A. A. Poot, *Regen. Med.*, 2014, **9**, 385-398.

- 32 P.-H. Chen, H.-C. Liao, S.-H. Hsu, R.-S. Chen, M.-C. Wu, Y.-F. Yang, C.-C. Wu, M.-H. Chen and W.-F. Su, *RSC Adv.*, 2015, **5**, 6932-6939.
- 33 S. M. Hasan, J. E. Raymond, T. S. Wilson, B. K. Keller and D. J. Maitland, *Macromol. Chem. Phys.*, 2014, **215**, 2420-2429.
- 34 C.-W. Ou, C.-H. Su, U.-S. Jeng and S.-h. Hsu, *ACS Appl. Mater. Interfaces*, 2014, **6**, 5685-5694.
- 35 A. Solanki, J. Mehta and S. Thakore, *Carbohydr. Polym.*, 2014, **110**, 338-344.
- 36 J. Fang, Q. Yong, K. Zhang, W. Sun, S. Yan, L. Cui and J. Yin, *J. Mater. Chem. B*, 2015, **3**, 1020-1031.
- 37 D. Liu, Z. Ma, Z. Wang, H. Tian and M. Gu, *Langmuir*, 2014, **30**, 9544-9550.
- 38 S. Pina, J. M. Oliveira and R. L. Reis, *Adv.Mater.*, 2015, **27**, 1143-1169
- 39 L. Yildirimer and A. M. Seifalian, *Biotechnol. Adv.*, 2014, **32**, 984-999.
- 40 Y. Zhang, N. Yao, F. Wang, W. Li and S. Jiang, *RSC Adv.*, 2014, **4**, 60007-60016.
- 41 Y. Yang, Y. Ning, C. Wang and Z. Tong, *Polym. Chem.*, 2013, **4**, 5407-5415.
- 42 Y. Wang, C. Zhang, Z Du, H. Li, W. Zou, *Synthe Met* 2013, **182**:49- 55.
- 43 C. Zhao, E. Danish, N. R. Cameron and R. Katakya, *J. Mater. Chem.*, 2007, **17**, 2446-2453.
- 44 E. Ruckenstein and J. S. Park, *Synth. Met.* 1991, **44**, 293-306.
- 45 E. Ruckenstein and J.-H. Chen, *Polymer*, 1991, **32**, 1230-1235.
- 46 K. Li, C. Zhang, Z. Du, H. Li, W. Zou, *Synth. Met.*, 2012, **162**, 2010- 2015
- 47 M. S. Silverstein, H. Tai, A. Sergienko, Y. Lumelsky and S. Pavlovsky, *Polymer*, 2005, **46**, 6682-6694.
- 48 P. J. Wilde, *Curr. Opin. Colloid Interface Sci.*, 2000, **5**, 176-181.
- 49 S. Yang, X. Zhang, H. Mi and X. Ye, *J. Power Sources*, 2008, **175**, 26-32.
- 50 M. Valcárcel, S. Cárdenas, B. M. Simonet, Y. Moliner-Martínez and R. Lucena, *TrAC, Trends Anal. Chem.*, 2008, **27**, 34-43.
- 51 K. A. Wepasnick, B. A. Smith, J. L. Bitter and D. H. Fairbrother, *Anal.Bioanal.Chem.*, 2010, **396**, 1003-1014.